*Asian Engineering Review*
*Vol. 5, No. 1, 1-7, 2018*
*ISSN(E) 2409-6725/ ISSN(P) 2518-0150*
*DOI: 10.20448/journal.508.2018.51.1.7*


# Laser Doppler Velocimetry of Rotating Cylinder with Retroreflecting Surface

**Gregory Dolya**[1]
**Kostiantyn Bondarenko**[2]

[1]*Professor, Department of Theoretical and Applied Systems Engineering, Faculty of Computer Science, V.N. Karazin Kharkiv National University, Kharkiv, Ukraine*
*Email: gdolya@ukr.net Tel: +38(057)7075022*
[2]*Student, Department of Systems and Technologies Modeling, Faculty of Computer Science, V.N. Karazin Kharkiv National University, Kharkiv, Ukraine*
*Email: konstantinb2016@gmail.com Tel: +38(099)0986668*


*(✉ Corresponding Author)*

## Abstract

A method for measuring rotation frequency of cylindrical object is considered, taking into account features of retroreflecting surface based on micro glass beads. Method involves single-beam object probing, detection of scattered radiation and spectral analysis of the recorded photocurrent. A mathematical model of the proposed method is described. Results of physical simulation are presented in form of plots, showing dependencies of received signal power on the frequency. Analysis of changes in registered photocurrent spectrum was done, taking into account both changes due to the vary of angular velocity of cylinder and those caused by rotation axis displacement in regard of falling light beam.

**Keywords:** Laser speckle-velocimetry, Doppler frequency, Retro reflective sheeting, Microscopic glass beads, Rotation frequency, Cylindrical objects.

**Citation** | Gregory Dolya; Kostiantyn Bondarenko (2018). Laser Doppler Velocimetry of Rotating Cylinder with Retroreflecting Surface. Asian Engineering Review, 5(1): 1-7.
**History:**
Received: 12 September 2018
Revised: 16 October 2018
Accepted: 22 November 2018
Published: 17 December 2018

**Publisher:** Asian Online Journal Publishing Group

**Contribution/Acknowledgement:** Both authors contributed to the conception and design of the study.
**Funding:** This study received no specific financial support.
**Competing Interests:** The authors declare that they have no conflict of interests.
**Transparency:** The authors confirm that the manuscript is an honest, accurate, and transparent account of the study was reported; that no vital features of the study have been omitted; and that any discrepancies from the study as planned have been explained.
**Ethical:** This study follows all ethical practices during writing.

## Contents

## 1. Introduction

Nowadays laser sensors are widely used for various purposes in such fields as scientific researches, industrial applications, remote control of the environment, etc [1, 2].

When irradiating an object, the light, which is scattered on a rough surface or on a set of particles in the flow, creates a specific speckle pattern, the analysis of which can be useful in controlling movement of the surface, determination of its quality or deformation, astronomical observations and other applications. One of such applications is the measurement of the objects motion velocity based on the correlation analysis. Depending on measuring device type, observed parameter can be a dynamically changing speckle pattern [3] or the motion velocity of individual particles in the flow [4] and, also, the Doppler shift of scattered laser radiation particles [5-8]. Last mentioned meters, called laser Doppler velocimetres (LDV), are now being used successfully to solve a number of applied problems.

Recently, for practical applications, a new class of retroreflective surfaces (RRS) has appeared, consisting of miniature retroreflectors based on either microprizms or glass beads [9] which make it possible to substantially increase the power of detected laser radiation. Their essential difference from rough surfaces or scattering particles in the flow is regularities of scattered radiation spatial distribution. With this difference in mind, a whole range of new efficient devices can be built, such as vibration sensors [10] or acoustic vibration sensors [11] as well as linear or angular motion velocity meters [12, 13] i.e laser velocimeters. In the paper [13] the analysis of the Doppler frequency of scattered laser radiation was used to describe the velocimeter work principles. The obtained results allow us to determine the rules for its construction and the features of practical implementation of LDV using RRS. Some experimental studies results and theoretical analysis of the constructing principles of an angular velocity meter using the interferometric approach are presented in Dolya, et al. [12]. But such an approach seems to have limitations, because it does not allow describing some essential features of the device. In the present paper to solve this problem we are using a method based on analysis of Doppler frequencies of scattered laser radiation on a rotating cylindrical object with RRS, which makes it possible to describe a broader series of regularities of devices operation for practical use.

## 2. Main Part

Fig. 1 shows the structure of the front-illuminated retroreflective surface containing a set of glass beads. As can be seen from the presented figure, the beads are located chaotically, they have an average diameter $d$ close to hundreds of micrometers.

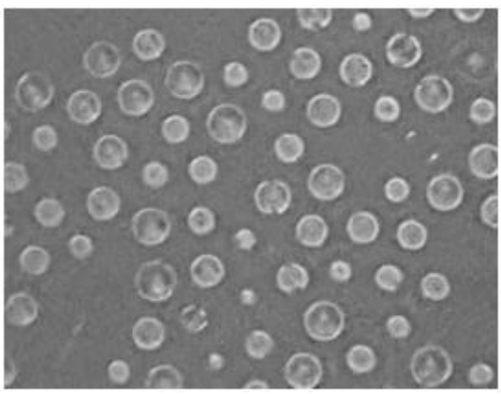

**Figure-1.** A sheet with microscopic glass beads

The diffraction pattern formed in the observation plane also has a random structure and changes as the object moves. Fig. 2.a shows the results of simulation modeling of the laser radiation diffraction process on the random implementation of RSS.

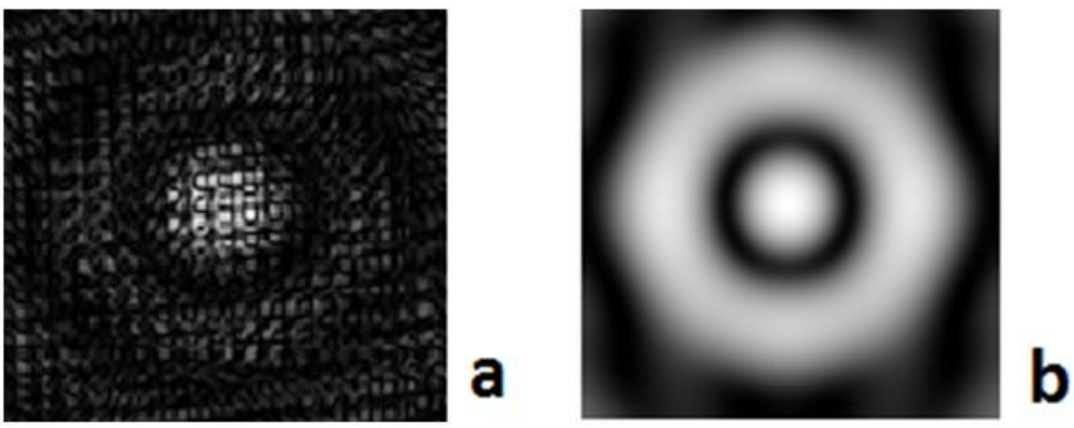


**Figure-2.** Results of simulation modeling of the laser radiation diffraction process

In Fig. 2.b the diffraction pattern averaged over the realizations is presented. The angular width of the maximum has magnitude of order $\lambda / d$ and is a few degrees in the characteristic observation conditions. Here $\lambda$ is the wavelength of the laser radiation.

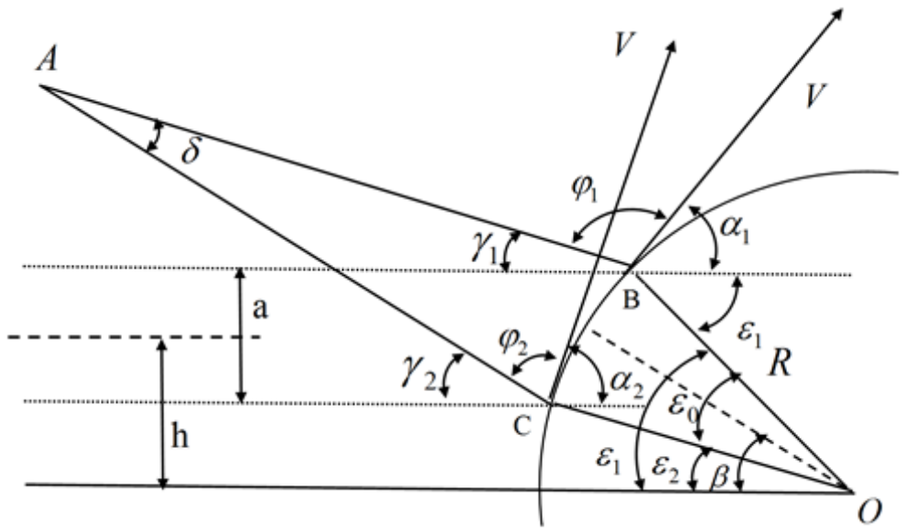


**Figure-3.** The scheme of beam falling on a rotating cylinder

To analyze the variation of the diffraction pattern in time via parameters, we use the scheme and notations shown in Fig. 3. We assume that a cylinder has a radius $R$ and, being covered with a retroreflective surface, rotates with a cyclic frequency $\nu$ about an axis that is perpendicular to the plane of the figure. The points on the surface have velocity $V = 2\pi\nu R$.

A laser beam of diameter $a$ with a plane wave front falls on the surface of the cylinder, the beam axis being a distance of $h$ from the direction to the axis of the cylinder. Diffuse (diffracted or scattered) radiation is observed at an arbitrary point $A$. All points within the illuminated region on the surface of the cylinder contribute to the observed intensity of laser radiation at the point $A$. For the sake of simplicity, we consider only the rays lying in the plane of the figure. Using the approach proposed in Dolya and Lytvynova [13] we can represent the dependence of the intensity at point $A$ on time in the form of expression

$$I(t) = \frac{1}{\lambda^2}\int_S E(\gamma_1, t)\exp\left[j2\pi f_1(\gamma_1)t\right]E^*(\gamma_2, t)\exp\left[j2\pi f_2(\gamma_2)t\right]d\gamma_1 d\gamma_2 . \quad (1)$$

Here $\gamma$ denotes the angle at which radiation is scattered to point $A$ from an arbitrary point within the illuminated region. It follows from the patterns of retroreflection that the amplitude of the field observed at the point $A$ is maximal in the case $\gamma = 0$ and substantially decreases for angles $\gamma$ greater than few degrees (Fig. 2a, b). This feature of laser radiation scattering by the RRS makes it significantly different from scattering by individual moving particle in applied anemometry problems [5, 6] and also from the case of the rough surface [7, 8]. The values of the amplitude $E$ are random (Fig. 2a) and depend on the realization of the surface at the observation time. The movement of the object causes intensity fluctuations in time, which are smoothed out when the object moves (averaging over the realizations).

Another factor that causes fluctuations in time is the difference in frequencies $f_1$ and $f_2$ in the ratio (1), due to the Doppler effect. These frequencies are different because on the surface of the cylinder there is a difference between the angles of incidence $\alpha$ and reflection $\varphi$ for different points. The expressions for the frequencies $f_1$ and $f_2$ have the form, respectively, for points on the periphery of the beam

$$f_1 = f\left[1 - \frac{V}{c}\left(\cos\alpha_1 - \cos\varphi_1\right)\right]; \quad (2)$$

$$f_2 = f\left[1 - \frac{V}{c}\left(\cos\alpha_2 - \cos\varphi_2\right)\right]. \quad (3)$$

If we integrate the intensity of the scattered radiation within the observation region and detect the received power, then the current at the output of the photo detector will also fluctuate in time with a continuous set of frequencies within the limits $f_1 - f_2$. Note that the value of $f_1 - f_2$ is maximal when the points contributing to the photocurrent are located on the periphery of the beam (points $C$ and $B$ in Fig. 3). In addition, we note that $f_1 - f_2 \to 0$ at $a \to 0$, since in this case the angular difference for the incident and reflected rays disappears.

We will estimate the range of Doppler frequencies arising when detecting laser radiation scattered on a rotating cylinder in more detail. We write the expression for the frequency difference in the form

$$f_1 - f_2 = \frac{fV}{c}\left(\cos\varphi_1 - \cos\varphi_2 + \cos\alpha_2 - \cos\alpha_1\right). \quad (4)$$

We consider separately the summands in the given relation. So

$$\cos\alpha_2 - \cos\alpha_1 = -2\sin\frac{\alpha_1 + \alpha_2}{2}\sin\frac{\alpha_1 - \alpha_2}{2} = -2\sin\frac{\pi - \varepsilon_1 + \varepsilon_2}{2}\sin\frac{\varepsilon_0}{2} = -2\cos\beta\sin\frac{\varepsilon_0}{2}. \quad (5)$$

In carrying out the transformations, obvious equalities were taken in mind

$$\alpha_{1,2} + \varepsilon_{1,2} = \frac{\pi}{2};$$

$$\alpha_1+\alpha_2=\pi-(\varepsilon_1+\varepsilon_2);$$
$$\alpha_1-\alpha_2+\varepsilon_1-\varepsilon_2=0.$$

Here it is also taken into account that

$$\varepsilon_1-\varepsilon_2=\varepsilon_0;$$
$$\frac{\varepsilon_1+\varepsilon_2}{2}=\beta,$$

which follows from the notation in Fig. 3.

We will transform the second term with an account of the following relations

$$\gamma_2=\gamma_1+\delta;$$
$$\gamma_{1,2}+\varphi_{1,2}+\alpha_{1,2}=\pi.$$

Consequently

$$\varphi_1+\varphi_2=2\pi-(\alpha_1+\alpha_2)-(\gamma_1+\gamma_2)=\pi-(\alpha_1+\alpha_2)+(\varepsilon_1+\varepsilon_2);$$
$$\varphi_1-\varphi_2=\varepsilon_0+\delta.$$

Therefore

$$\begin{aligned}
&\cos\varphi_1-\cos\varphi_2=-2\sin\frac{\varphi_1+\varphi_2}{2}\sin\frac{\varphi_1-\varphi_2}{2}=\\
&=-2\sin\frac{\pi-(\gamma_1+\gamma_2)+(\varepsilon_1+\varepsilon_2)}{2}\sin\frac{\varepsilon_0+\delta}{2}=\\
&=-2\cos\left(\frac{\gamma_1+\gamma_2}{2}-\beta\right)\sin\frac{\varepsilon_0+\delta}{2}=\\
&=-2\left(\cos\frac{\gamma_1+\gamma_2}{2}\cos\beta+\sin\frac{\gamma_1+\gamma_2}{2}\sin\beta\right)\left(\sin\frac{\varepsilon_0}{2}\cos\frac{\delta}{2}+\cos\frac{\varepsilon_0}{2}\sin\frac{\delta}{2}\right)=\\
&=-2\left(\cos\frac{\gamma_1+\gamma_2}{2}\cos\beta+\sin\gamma_0\sin\beta\right)\left(\sin\frac{\varepsilon_0}{2}\cos\frac{\delta}{2}+\cos\frac{\varepsilon_0}{2}\sin\frac{\delta}{2}\right)=\\
&=-2\left(\cos\beta+\sin\frac{\gamma_1+\gamma_2}{2}\sin\beta\right)\left(\frac{a}{2R}+\frac{a}{2L}\right).
\end{aligned}\qquad(6)$$

In the derivation of the last relation, the smallness of the angular quantities was taken in account

$$\sin\frac{\delta}{2}\approx\frac{a}{2L};$$
$$\cos\frac{\delta}{2}\approx1;$$
$$\sin\frac{\varepsilon_0}{2}\approx\frac{a}{2R};$$
$$\cos\frac{\varepsilon_0}{2}\approx1,$$

which follows from the statement of the problem assuming that the size of the laser beam is much smaller than the cylinder radius, and the observation point is sufficiently far from the illuminated region. In addition, it is also taken into account, that a significant contribution to the spectrum of the observed Doppler frequencies is made by rays with $\gamma \square\ 1$, which follows from the properties of retroreflection. Therefore, we can assume that $\cos\frac{\gamma_1+\gamma_2}{2}\approx1.$

The above relations enable us to represent the equality (4) in the form

$$f_1-f_2=\Delta f+\delta f,\qquad(7)$$

where

$$\Delta f=\frac{2fVa}{cR}\cos\beta\left(1+\frac{R}{2L}\right),\qquad(8)$$

and

$$\delta f=\frac{fV}{c}\sin\frac{\gamma_1+\gamma_2}{2}\sin\beta\left(\frac{a}{R}+\frac{a}{L}\right).\qquad(9)$$

Expression (7) makes it possible to estimate the width of the range of Doppler frequencies arising in the photocurrent spectrum upon detection of laser radiation scattered by a rotating cylinder with RRS. As can be seen, these frequencies are concentrated in two ranges, which have a different nature of dependency on the conditions of observation. Let us first consider the case when a laser beam hits the surface of a cylinder in a direction passing through the center of the cylinder, i.e. in the case when $h=0$. In this case $\beta=0$; $\sin\beta=0$ and $\delta f=0$. Then in the spectrum of Doppler frequencies there will be frequencies present only in the range of $\Delta f$

$$\Delta f=\frac{4\pi va}{\lambda}\left(1+\frac{R}{2L}\right).\qquad(10)$$

Here it is taken in account, that $V = 2\pi\nu R$, where $\nu$ is cylinder rotation frequency, and that $f/c = 1/\lambda$.

Analyzing this ratio, it can be noted that for $a \to 0$, $\Delta f \to 0$, which has obvious physical meaning and has already been discussed above. In addition, if the observation plane is sufficiently far from the cylinder, then $R \ll L$ and the Doppler frequency band does not depend on the radius of the cylinder. We note that this fact was confirmed experimentally in Dolya, et al. [12]. Also, it should be expected that the band of observed Doppler frequencies should increase with increasing angular velocity of the object $\nu$.

To verify the last statement and for making subsequent conclusions from the analysis of the obtained relations, an experimental setup was assembled, the scheme of which is shown in Fig. 4.

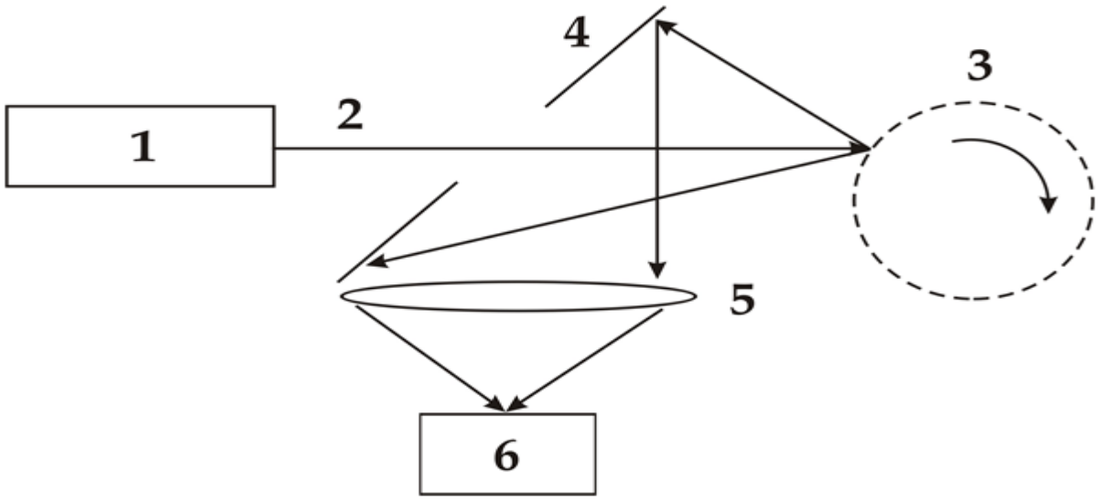


**Figure-4.** The scheme of experimental setup

Here the numbers denote: 1 - solid green laser, 2 - beam incident on 3 - cylinder with RRS, 4 - mirror with a hole in the middle, 5 - lens, 6 - photo detector. The current of the photodetector, which occurs when the laser radiation scattered on a rotating cylinder is detected, was digitized and obtained spectrum was analyzed. For an experimental estimate of the magnitude of the range, the laser beam was directed to the cylinder surface in such a way, that the condition $h = 0$ was satisfied. It was expected that the value of $\delta f$ would be a zero, as follows from relation (9).

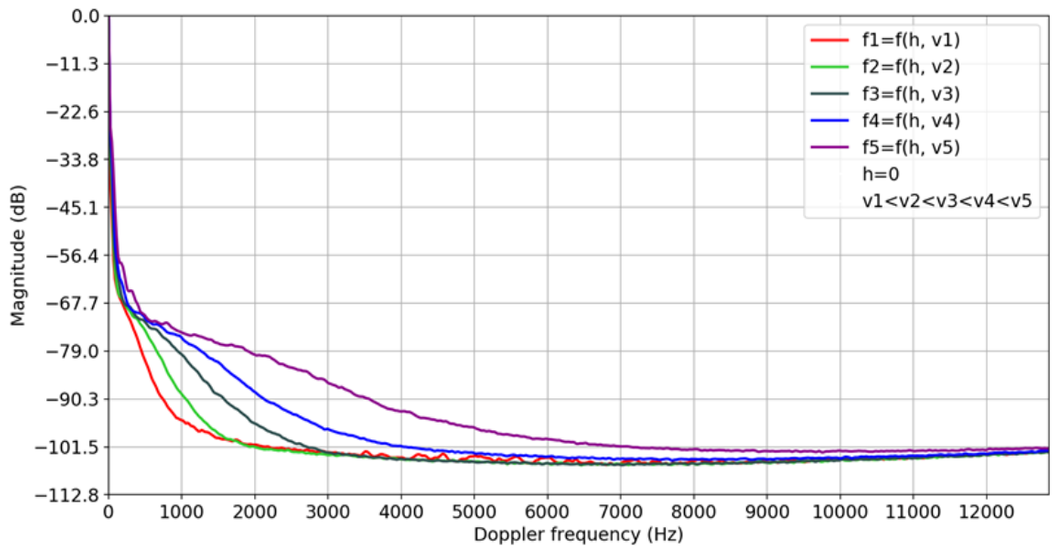


**Figure-5.** Dependence of photocurrent spectrum width on rotation frequency

The results of an experimental study of the width of the spectrum of Doppler frequencies are shown in Fig. 5. On the horizontal axis, the values of the amplitudes of Doppler frequencies are plotted. On the vertical axis, the values are the frequencies of photocurrent fluctuations proportional to the power of the detected light. In order to avoid the influence of fluctuations in the photocurrent, due to the dynamically changing structure of the RR surface during its motion within the illuminated region, the recorded photocurrent was averaged over time.

The figure shows a set of curves obtained for different values of the angular velocity of rotation $\nu$. It can be seen from these curves that the maximum amplitude of Doppler frequencies is observed at the beginning of the spectral range and decreases with increasing of Doppler frequencies. This can be explained by the fact, that the maximum amplitude of the light waves $E$ is observed at angles $\gamma$ close to zero. In addition, it can be seen from these graphs, that a greater width of the spectral range $\Delta f$ corresponds to a greater frequency of cylinder rotations around the axis $\nu$, which corresponds to the theoretical analysis results (relation (8)).

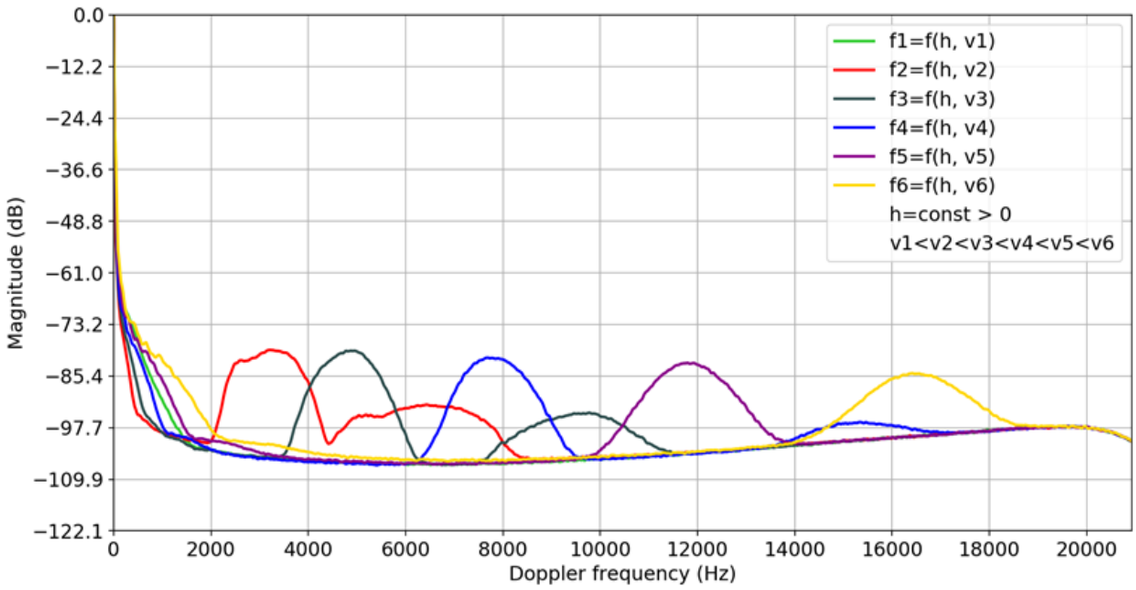


**Figure-6.** Dependence of photocurrent spectrum on $\nu$

The next stage in the experimental studies was the study of the dependence of the ranges $\Delta f$ and $\delta f$ for the case $h \neq 0$ when the observation conditions were changed. One of the research results is shown in Fig. 6. Curves 1-5 were obtained with increasing angular velocity $\nu$ for a fixed value of $h$. From these curves, it is seen that as the $\nu$ increases, spectral range $\delta f$ expands, with all frequencies within this range shifting toward higher frequencies. It is interesting to note that along with the main range $\delta f$ for curves 1-3, an additional spectral range at the doubled frequency is clearly noticeable. This is due to the interaction of waves spreading to different points, which are symmetric with respect to the beam axis in the forward and backward directions in regard to the motion velocity vector. It is also seen that the character of the change of the range $\delta f$ from the angular velocity $\nu$ is in good agreement with the theoretical analysis results, despite a number of limitations accepted in the theoretical analysis in this scheme of laser velocimetry.

It is also worthwhile to pay attention to the low-frequency range of the spectral distribution of the Doppler frequencies in Fig. 6, which corresponds to the range $\Delta f$ considered above. Its value in this case is described by the relation

$$\Delta f = \frac{4\pi\nu a}{\lambda}\left(1+\frac{R}{2L}\right)\sqrt{\left(1-\frac{h^2}{R^2}\right)}. \qquad (11)$$

As can be seen from the Fig. 6, in this case with $h \neq 0$, as well as with $h = 0$, the range $\Delta f$ broadens with increasing the value of $\nu$, that matches well with relation (11).

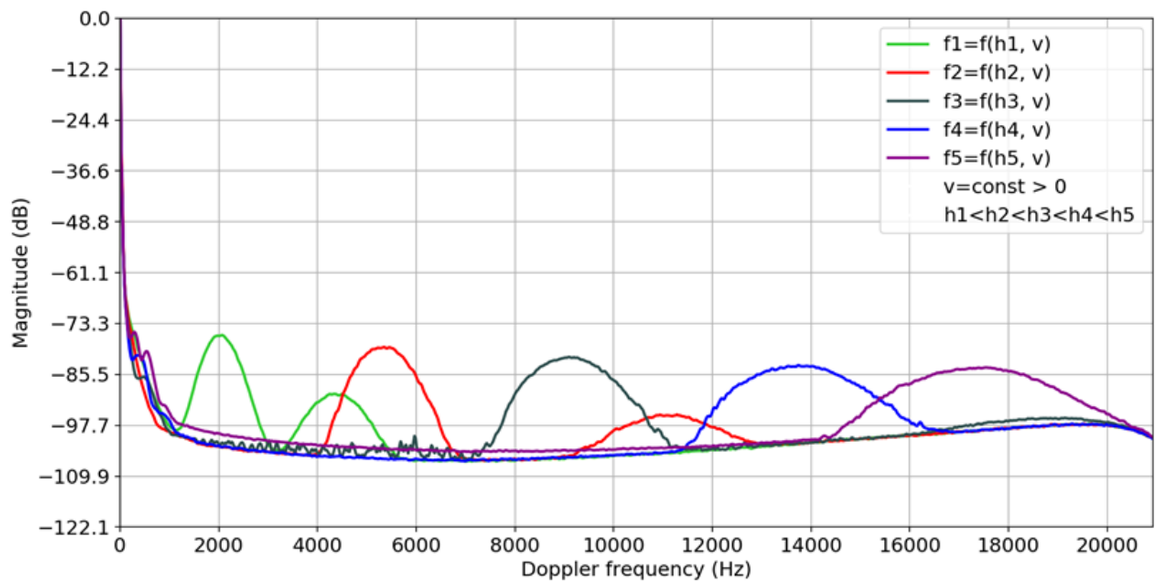


**Figure-7.** Dependence of photocurrent spectrum on $h$

Fig. 7 shows the results of experimental studies of the Doppler frequencies spectrum for a fixed $\nu$ value, but a variable value of the parameter $h$. Curves 1-5 correspond to an increase in the value of $h$. It follows from (9) that

$$\delta f = \frac{2\pi\nu h}{\lambda}\sin\frac{\gamma_1+\gamma_2}{2}\sin\varepsilon_0\left(1+\frac{R}{L}\right). \qquad (12)$$

This means that as the value of $h$ increases, the regularities of the change in the frequencies $\delta f$ are analogous to the dependences obtained when $v$ is varied, i.e. with increasing $v$, the spectral range $\delta f$ expands, and all frequencies inside it are shifted towards increasing frequency as the value of the parameter $h$ increases. Analysis of the course of the dependencies in Fig. 7 shows that the experimental studies results are in good agreement with the results of the theoretical analysis.

Analyzing the relation (11), it can be noted that when changing the parameter $h$, we should expect a change in the value of $\Delta f$, although it is rather weak for small values of $h$. This conclusion corresponds to the nature of the change in the spectrum of Doppler frequencies in the low-frequency region in Fig. 7. It can be seen that the curves obtained for different values of $h$ are practically indistinguishable, in contrast to the character of the dependencies of the spectra in the low-frequency region in Fig. 6.

Analyzing the relations (8) and (9), we can note that $\Delta f \sim V\cos\beta$ and $\delta f \sim V\sin\beta$. This means that the appearance of Doppler frequencies within $\Delta f$ is due to the transverse to the ray projection of the point's velocity on the cylinder. Similarly, the frequencies within the limits of $\delta f$ are due to the longitudinal component of the velocity. From the results of the theoretical analysis (relations (8) and (9)) and experimental studies (curves in Fig. 5-7) it follows that the component of the velocity of the cylinder surface transverse to the beam leads only to an expansion of the Doppler frequencies spectrum, while the presence of the longitudinal component leads to the appearance of second frequency range with their own, different from the first, properties. Here we can also state a good correspondence between the results of theoretical analysis and experimental studies.

It should be noted that the last conclusions made are analogous to those made in [16] for the features of laser Doppler velocimetry of planar objects moving rectilinearly.

## 3. Conclusions

In this paper we consider a method for measuring frequency of cylindrical object rotation, taking into account the features of retroreflecting surface containing a set of micro glass beads. The method is based on single-beam object probing, detection of scattered radiation, and spectral analysis of the recorded photocurrent. The spectral distribution has a noticeable correlation with the value of the cylinder rotational velocity, which is the basis of its practical use. A theoretical analysis of the spectral distribution features is done. It is based on the description of the Doppler shift regularities of the laser radiation frequencies on a moving surface. The experimental studies results and theoretical analysis are in good agreement, which confirms the validity of conclusions made.

## References


[1] R. M. Measures, *Laser remote sensing: Fundamentals and applications*. Malabar, Florida: Krieger Publishing Company, 1992.
[2] T. Fukuchi and T. Shiina, *Industrial applications of laser remote sensing*: Bentham Science Publishers, 2012.
[3] M. Kowalczyk, "Laser speckle velocimetry," in *Optical Velocimetry, SPIE Proceedings*, 1996, pp. 139–145.
[4] M. Raffel, C. Willert, and J. Kompenhans, *Particle image velocimetry. A practical guide*: Springer, 1998.
[5] M. Alaimo, D. Magatti, F. Ferri, and M. Potenza, "Heterodyne speckle velocimetry," *Applied Physics Letters*, vol. 88, p. 191101, 2006.
[6] B. S. Rinkevichius, *Laser diagnostic in fluid mechanics*. Moscow: Moskow Power Engineering Institute Publication, 1998.
[7] S. S. Ulyanov, "Dynamics of speckles with a small number of scattering events: Specific features of manifestation of the Doppler effect," *Applied Optics*, vol. 53, pp. B94-B102, 2014.
[8] S. S. Ulyanov, "Speckle dynamics and doppler effect," *ISSEP Journal*, vol. 7, pp. 1-7, 2001.
[9] J. Lloyd, *A brief history of retroreflective sign face sheet materials the principles of retroreflection*: REMA Publications, 2008.
[10] G. N. Dolya and V. Zhyvchuk, "The appreciation of the influence of exactness of focusing on the work of the laser homodyne method of measuring the parameters of vibration," in *SPIE Proceedings*, 2004, pp. 45-52.
[11] G. N. Dolya and E. S. Litvinova, "Retroreflective laser detector of acoustic oscillations," in *Proceedings of 12th International Conference on Laser & Fiber-Optical Networks Modeling (LFNM'2016)*, 2016, pp. 108-111.
[12] G. N. Dolya, A. N. Katunin, O. A. Nad, and A. N. Bulay, "Laser speckle velocimetry for running objects with light reflective surface," *Systems of Information Processing, Kharkiv, KhUAF*, vol. 1, pp. 23-26, 2015.
[13] G. Dolya and O. Lytvynova, "Modeling the method of laser doppler speckle-velocimetry for flat objects with retroreflective surface," *Asian Engineering Review*, vol. 4, pp. 7-13, 2017.Available at: https://doi.org/10.20448/journal.508.2017.42.7.13.